Application of an Ensemble Kalman Filter With Gaussian Anamorphosis to a 1D Detonation Flow

James J. Hansen[a], Davy Brouzet[b], Matthias Ihme[b,c]

[a]Department of Aeronautics & Astronautics, Stanford University
Stanford, California, United States of America

[b]Department of Mechanical Engineering, Stanford University
Stanford, California, United States of America

[c]Department of Photon Science, SLAC National Accelerator Laboratory
Menlo Park, California, United States of America

1 Introduction

Pressure-gain propulsion systems, such as rotating detonation engines, depend heavily on detonation phenomena for their operation. However, rigorously modeling detonation behavior under realistic operating conditions presents significant challenges. Interactions between shock waves, chemical reactions, and turbulent flow fields are highly nonlinear, making predictions sensitive to initial and boundary conditions as well as modeling choices. Additionally, collecting comprehensive experimental datasets to inform these models is inherently complex. The flow fields often feature extreme pressures, high temperatures, and very short timescales. Using statistical methods to integrate available experimental data into numerical models could therefore help improve our confidence in simulation results and accelerate discovery.

Data assimilation (DA) techniques combine observational data with numerical simulations to improve state and parameter estimates. These methods originated in the numerical weather prediction community, where they have proven highly effective in integrating sparse observations into large models with complex, nonlinear dynamics [1]. Recently, studies have explored the use of DA in predicting shock flows. Hansen et al. (2024) and Houba et al. (2024) integrated sequential data assimilation methods with numerical schemes to improve shock resolution in non-reacting flows with discontinuities [2, 3], and West et al. (2025) used a variational data assimilation approach to treat one-dimensional shock-laden flows [4]. These developments suggest that similar methods could be adapted to detonations; however, DA has not yet been applied in this context.

This work seeks to address this gap by applying sequential data assimilation to a one-dimensional detonation simulation, aiming to demonstrate how DA can improve state estimates and reduce uncertainties in quantities of engineering interest.

Correspondence to: jjhansen@stanford.edu

2 Computational Approach

2.1 The NS-EnKF Algorithm

Data assimilation is performed using a variant of the ensemble Kalman filter (EnKF) initially introduced by Evensen for large-scale numerical models [5]. The EnKF employs an analysis step that approximates the Kalman filter for linear and Gaussian systems. Error covariance matrices are estimated from a finite set of model state realizations, referred to as ensemble members. These realizations are propagated using the full system model, with updates applied as observations become available. The EnKF analysis step, performed on each of the ensemble members, is given by

$$\mathbf{\Phi}^{\mathrm{a}} = \mathbf{\Phi}^{\mathrm{f}} + \mathbf{P}^{\mathrm{e}}\mathbf{H}^{\mathrm{T}}\left[\mathbf{H}\mathbf{P}^{\mathrm{e}}\mathbf{H}^{\mathrm{T}} + \mathbf{R}^{\mathrm{e}}\right]^{-1}(\mathbf{y} - \mathbf{H}\phi^{\mathrm{f}}), \tag{1}$$

where $\mathbf{\Phi}^{\mathrm{f}}$ and $\mathbf{\Phi}^{\mathrm{a}}$ are the forecast and analysis state vectors, $\mathbf{y}$ is the vector of observations, $\mathbf{P}^{\mathrm{e}}$ and $\mathbf{R}^{\mathrm{e}}$ are the ensemble-based state and measurement error covariance matrices, and $\mathbf{H}$ is the observational operator.

The EnKF relies on the assumption that uncertainties are Gaussian distributed such that all probability distribution functions can be described completely by their first and second moments. When applied to systems with non-Gaussian distributed errors, the EnKF analysis can yield suboptimal results and amplify instabilities [6]. This issue is particularly relevant in systems involving shock flows. An example of how non-Gaussian state distributions materialize in a shock flow is illustrated in Fig. 1, where probes show the distribution of pressure in an ensemble of detonation simulations. There is uncertainty in the true location of the shock, and the pressure distribution is strongly bimodal.

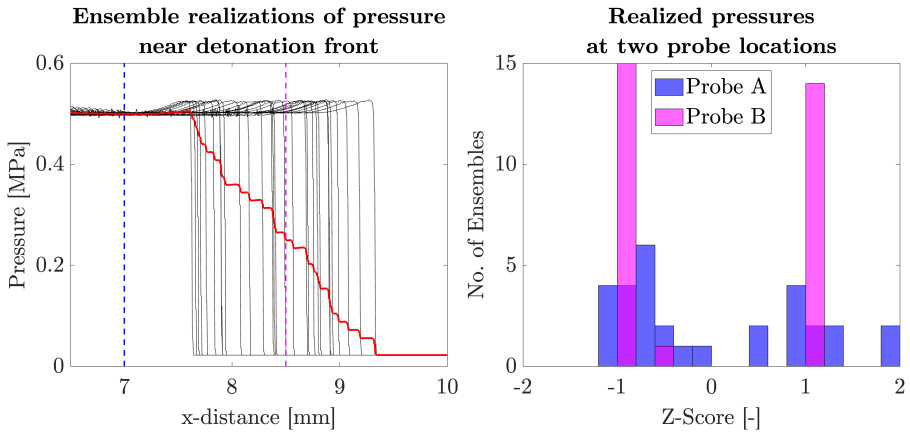

Figure 1: Left: An ensemble of pressure profiles near the detonation front of a 1D simulation. The ensemble mean is in red. Probe A is located at 7.0 mm and Probe B is located at 8.5 mm. Right: Histograms of the distributions of pressure at both probes. At Probe B, the pressure is bimodally distributed.

To address these limitations, Zhou et al. [7] introduced the normal-score EnKF (NS-EnKF), which modifies the EnKF with a Gaussian anamorphosis. A transfer function $\mathcal{F}$, based on the cumulative distribution function of the forecast state vector, is constructed such that

$$\widehat{\mathbf{\Phi}}^{\mathrm{f}}, \widehat{\mathbf{y}} = \mathcal{G}^{-1}[\mathcal{F}(\mathbf{\Phi}^{f}, \mathbf{y})], \tag{2}$$

where $\mathcal{G}$ is the cumulative distribution function for the standard normal distribution. This transformation enforces a marginal Gaussian distribution on the joint state and observation vector, ensuring the Gaussian assumption is satisfied. The EnKF update is then performed with $\widehat{\mathbf{\Phi}}^{\mathrm{f}}$ and $\widehat{\mathbf{y}}$ used in place of $\mathbf{\Phi}^{\mathrm{f}}$ and $\mathbf{y}$.

Prior to continuation of the forecast, the updated state vector is brought back into the original space using an inverse transformation,

$$\mathbf{\Phi}^{\mathrm{a}} = \mathcal{F}^{-1}[\mathcal{G}(\widehat{\mathbf{\Phi}}^{a})]. \tag{3}$$

Use of a normal-score transform enhances the filter's performance when applied to systems involving non-Gaussian or chaotically evolving error distributions. Details on the construction of the transfer function and application of this transform to shock flows can be found in Hansen et al. [2].

2.2 Numerical Methods

In our DA approach, we construct an ensemble of 30 one-dimensional detonation simulations. The ensemble's initial conditions are generated stochastically. A 1D domain is initialized with a stationary $CH_4/O_2/N_2$ mixture at an equivalence ratio of $\phi = 1$ and a 25% N_2 molar dilution. The initial temperature and pressure of this mixture are $T_u = 300$ K and $p_u = 22.2$ kPa, respectively. The planar ZND solution for this mixture, computed using the SDToolbox by Brown et al. [8], is superimposed on the left side of the domain. The initial location of the right-moving detonation is randomly distributed as $\Delta x \sim \mathrm{Unif}(15, 35)$ mm. The domain has a streamwise length of $L_x = 250$ mm and is discretized uniformly using a Cartesian mesh with $N_x = 5,000$ cells, resulting in a uniform spacing of $50\,\mu\mathrm{m}$. This resolution corresponds to more than 60 cells per ZND induction length. Symmetry conditions are applied at the transverse boundaries, while non-reflecting boundary conditions are enforced at the streamwise ends.

A compressible, finite-volume code is used to solve the Navier-Stokes conservation equations for mass, momentum, energy and species, written with density ρ, gas velocity vector $\mathbf{u}$, pressure p and specific total energy e_t, and the mass fractions and source terms for species k being denoted by Y_k and $\dot{\omega}_k$, respectively:

$$\partial_t \rho + \nabla \cdot (\rho \boldsymbol{u}) = 0 \tag{4}$$

$$\partial_t (\rho \boldsymbol{u}) + \nabla \cdot (\rho \boldsymbol{u}\boldsymbol{u}) = \nabla \cdot (\boldsymbol{\tau} - p\boldsymbol{I}), \tag{5}$$

$$\partial_t (\rho e_t) + \nabla \cdot [\boldsymbol{u}(\rho e_t + p)] = \nabla \cdot [(\boldsymbol{\tau} \cdot \boldsymbol{u}) - \boldsymbol{q}], \tag{6}$$

$$\partial_t (\rho Y_k) + \nabla \cdot (\rho \boldsymbol{u} Y_k) = -\nabla \cdot \boldsymbol{j}_k + \dot{\omega}_k. \tag{7}$$

Species equations are solved for $k = 1$ to $N_s - 1$, where N_s is the number of species and N_2 is the last species. Formalisms for spatial discretization and time-advancement, as well as modeling of the stress tensor $\boldsymbol{\tau}$, heat flux $\boldsymbol{q}$ and diffusion flux for the kth species $\boldsymbol{j}_k$, follow those described in Brouzet et al. (2023) [9]. The system is closed with the ideal gas equation of state, and the chemical mechanism used is a 20-species, 97-reaction skeletal derivative [10] of the GRI3.0 mechanism for methane–air combustion.

2.3 Configuration

In this study, a Gaussian anamorphosis is combined with the stochastic EnKF implementation from the Parallel Data Assimilation Framework (PDAF) developed by Nerger and Hiller [11] to construct a NS-EnKF. Assimilation is then performed on the numerical models described in Section 2.2. Before the first assimilation update, ensemble model realizations are advanced to $t = 18.75\,\mu$s. Simulated observations of density ρ and the mass fractions of hydroxyl radical OH and formaldehyde CH_2O are then integrated at an observation rate of approximately 267 kHz.

Observations are obtained from an additional, equivalently constructed model realization, advanced to $t = 26.25\,\mu$s, and uniformly sampled every 20 cells, yielding $m = 251$ observations per flow state

variable at each observation time step. Before each update, min-max normalization is applied to the joint state and observation vector. The observation operator $\mathbf{H}$ in the EnKF update equation is defined to propagate information from observed to unobserved states. Observations of ρ and OH and CH_2O mass fraction are used to inform the update of all state vector quantities except the transverse velocity U_y. Quantities are grouped based on the qualitative features of each state variable. These groupings are listed below in Table 1. The universal observational error covariance is specified as 0.01, and neither covariance localization nor inflation is applied.

Table 1: Feature relationships prescribed in the observation operator $\mathbf{H}$.

Observed Quantity	Informed Quantity
ρ	ρ
OH	U_x, T, CH_4, H_2O, O_2, H_2, CO, CO_2, OH, H, O
CH_2O	CH_3, HO_2, C_2H_4, C_2H_5, C_2H_6, CH_2, CH_2(S), HCO, CH_2O, CH_3O

3 Results and Discussion

Results are now presented on the forecast and analysis time series for select flow state variables. First, the evolution of ensemble variance over time is studied as a surrogate for state uncertainty. Then, observations are made on the change in whole-field errors with assimilation and simulation advancement.

3.1 Evolution of Ensemble Variance

Figure 2 shows traces of ensemble variance over time. The statistic is constructed by taking the natural logarithm of the mean standard deviation across the domain and the ensemble. Six quantities are shown. The first three, ρ, Y_{CH_2O} and Y_{OH} are observed quantities, and the last three, T, Y_{CH_3} and Y_{H_2O} are unobserved quantities of interest. Dotted lines show the initial uncertainty for each quantity, and three assimilation updates are shown.

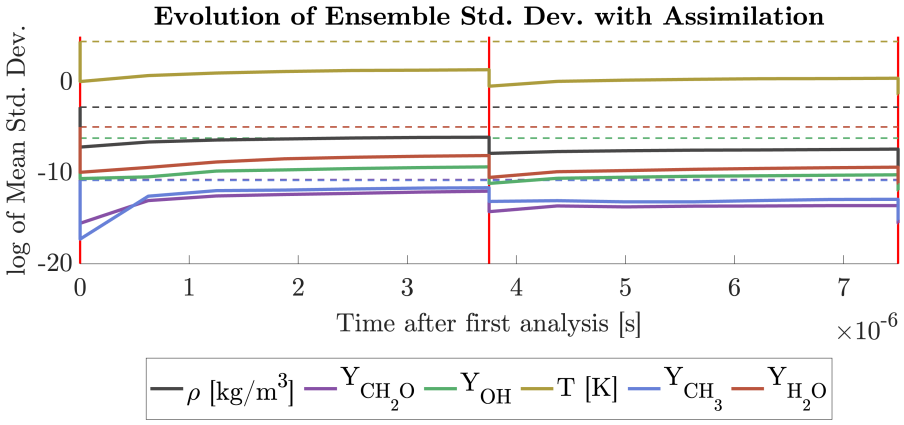

Figure 2: Evolution of the log-transformed mean standard deviation of different quantities over time. Initial values are shown with dotted lines. Three assimilations occur, indicated by vertical red lines.

Initial uncertainties in each flow state variable vary by quantity. As intermediate reaction species such as CH_2O and CH_3 have mass fractions of zero in most of the domain, their uncertainties in those regions and therefore on average are low. By contrast, temperature and density have larger areas of initial variance and therefore larger initial uncertainty.

The first assimilation update immediately lowers the uncertainty of all quantities, as is expected in the EnKF update [6]. Uncertainty then rebounds as the ensembles begin to diverge. Subsequent assimilations progressively lower uncertainty, and the final ensemble spreads are lower than at initialization. A steady net decrease in uncertainty is a desired result, as a complete collapse in ensemble variance would indicate the DA method is unable to further improve on the forecast solution.

3.2 Evolution of Mean Errors

The evolution of error in the same flow state variables with respect to the reference solution is illustrated below in Fig. 3. The error statistic is constructed by taking natural logarithm-transformed mean absolute percent error (MAPE) of the mean ensemble quantities. As in Fig. 2, initial error quantities are shown with dotted lines and three assimilations are performed.

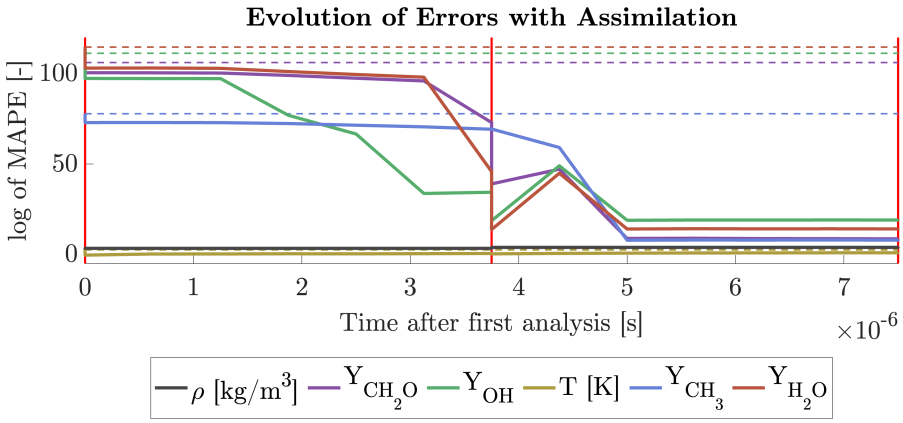

Figure 3: Evolution of the log-transformed mean absolute percent errors of different quantities over time. Initial error values are shown with dotted lines. Three assimilations occur, indicated by vertical red lines.

Initial errors are also differentiated by quantity. However, temperature and density have relatively low percentage errors except near the detonation front, while large percentage errors are present for species quantities. The first assimilation update provides a relatively small decrease in the ensemble error statistic, and large decreases are only seen after the second assimilation. The mean quantity errors then stabilize through the end of the calculation. It is notable that the assimilation algorithm decreases ensemble errors in both observed and unobserved quantities.

4 Conclusions

This study applies an ensemble Kalman filter with Gaussian anamorphosis stochastically initiated simulations of 1D methane-air detonation. Simulated observations of density and mass fractions of hydroxyl radical and formaldehyde are used in multiple sequential updates. Results indicate that feature information is propagated from observed to unobserved quantities as desired, and that mean errors are reduced with assimilation. However, work exploring additional error statistics over longer timescales is needed to prove the robustness of this method.

Acknowledgments

This material is based upon work supported by the National Science Foundation Graduate Research Fellowship under Grant No. DGE-1656518. We also acknowledge computing resources from the U.S. Department of Energy, National Nuclear Security Administration under award No. DE-NA0003968.

References

[1] Carrassi, A., Bocquet, M., Bertino, L. & Evensen, G. Data assimilation in the geosciences: An overview of methods, issues, and perspectives. *Wiley Interdisciplinary Reviews: Climate Change*. **9**, e535 (2018)

[2] Hansen, J., Brouzet, D. & Ihme, M. A Normal-Score Ensemble Kalman Filter for 1D Shock Waves. *AIAA SCITECH 2024 Forum*. 2024-1022 (2024)

[3] Houba, T., Edoh, A., Munipalli, R. & Harvazinski, M. Sequential Data Assimilation in Flows with Shocks. *AIAA SCITECH 2024 Forum*. 2024-0587 (2024)

[4] West, E., MacArt, J. & Munipalli, R. Variational Data Assimilation in Shock Tube Flows. *AIAA SCITECH 2025 Forum*. 2025-1166 (2025)

[5] Evensen, G. Sequential data assimilation with a nonlinear quasi-geostrophic model using Monte Carlo methods to forecast error statistics. *Journal Of Geophysical Research: Oceans*. **99**, 10143-10162 (1994)

[6] Evensen, G. The ensemble Kalman filter for combined state and parameter estimation. *IEEE Control Systems Magazine*. **29**, 83-104 (2009)

[7] Zhou, H., Gomez-Hernandez, J., Franssen, H. & Li, L. An approach to handling non-Gaussianity of parameters and state variables in ensemble Kalman filtering. *Advances In Water Resources*. **34**, 844-864 (2011)

[8] Browne, S., Ziegler, J., Bitter, N., Schmidt, B., Lawson, J. & Shepherd, J. SDToolbox: Numerical tools for shock and detonation wave modeling. *Explosion Dynamics Laboratory. GALCIT Report FM2018*. **1** (2018)

[9] Brouzet, D., Vignat, G. & Ihme, M. Dynamics and structure of detonations in stratified product-gas diluted mixtures. *Proceedings Of The Combustion Institute*. **39**, 2855-2864 (2023)

[10] Ma, P., Wu, H., Labahn, J., Jaravel, T. & Ihme, M. Analysis of transient blow-out dynamics in a swirl-stabilized combustor using large-eddy simulations. *Proceedings Of The Combustion Institute*. **37**, 5073-5082 (2019)

[11] Nerger, L. & Hiller, W. Software for ensemble-based data assimilation systems—Implementation strategies and scalability. *Computers Geosciences*. **55** pp. 110-118 (2013)